LA-UR- 04- 0106

Approved for public release;
distribution is unlimited.

Title: VUV and Soft X-ray Spectroscopy of Actinides

Author(s): Clifford G. Olson, Ames Lab; John J. Joyce, 108919,
Tomasz Durakiewicz, 171535, Elzbieta Guziewicz, 185963,
MST10

Submitted to: Materials Research Society Proceedings

Los Alamos
NATIONAL LABORATORY

VUV and Soft X-ray Spectroscopy of Actinides

Clifford G. Olson, John J. Joyce[1], Tomasz Durakiewicz[1], Elzbieta Guziewicz[1] andxxx
Ames Laboratory, Iowa State University, Ames, Iowa 50011
[1]Los Alamos National Laboratory, Los Alamos, New Mexico 87545

ABSTRACT

Optical and photoelectron spectroscopies using VUV and Soft X-ray photons are powerful tools for studies of elemental and compound actinides. Large changes in the relative atomic cross sections of the *5f*, *6d* and *sp* electrons allow decomposition of the character of the valence bands using photoemission. Resonant enhancement of photoelectrons and Auger electrons at the 5*d* core threshold further aids the decomposition and gives a measure of elemental specificity. Angle-resolved photoemission can be used to map the momentum dependence of the electronic states. The large changes in relative cross section with photon energy yields further details when the mapping is done at equivalent points in multiple zones. Spectra for well understood rare earth materials will be presented to establish spectral characteristics for known atomic character initial states. These signatures will be applied to the case of USb to investigate *f-d* hybridization near the Fermi level.

INTRODUCTION

As materials and light source accessibility issues are resolved, the power of vacuum ultra-violet (VUV) and soft X-ray photoemission can increasingly be applied to actinides. Modern high-resolution angle-resolved photoemission has been very effective in studying the states that form the Fermi surface in cuprate superconductors. With a broad range of photon energies, the same techniques can be applied to the more difficult three dimensional compounds. At the same time, the photon energy dependences can provide a wealth of information about the nature of the states involved. Spectra at equivalent momenta in different zones can be compared to see the effect resulting from the change in photon energy due to the changes in atomic cross sections. Strong resonant emission from *d* cores emphasizes the rare earth or actinide states. Details of the resonant spectra show the effects of hybridization. In many ways, the rare earths give "cleaner" examples of resonant behavior than the actinides. The whole rare earth system is available, and the greater overlap of the 4*f* and 4*d* wave functions make resonant behavior more detailed. For the most part, the lessons of the rare earths can be applied to the actinide series.

In what follows we will look at the spectral characteristics that allow us to determine that the states at and near the Fermi level of USb have mixed Uranium 5*f* and 6*d* character.

Cross sections

Calculated atomic cross sections from Yeh and Lindau [1] are traditionally invoked in attempts to use photoemission spectra to identify the parentage of electronic states. With the extra features (or complications) of f compounds, it is appropriate to ask under what conditions the atomic calculations apply. After all, these are excitation or absorption cross sections not emission probabilities. The model doesn't predict, for example, the extreme intensity modulations through resonance.

A very simple case to look at for rare earth emission cross sections are the rare earth trifluorides such as CeF_3. The Ce atom is coplanar with three F atoms, and there is a F above and below the Ce. All the Ce - F distances are approximately equal. In effect, the Ce atoms are matrix isolated. Other than dipole forbidden *f-f* transitions, this is a large gap insulator.

Figure 1 shows two Energy Distribution Curves (EDCs) of a thin film of CeF_3. The small Fermi step is from the metallic substrate. The 90 eV EDC is below the 4*d*-4*f* resonance and the 120 eV EDC is in the main resonance peak. The advantage of CeF_3 is that the states of differing atomic character are well separated so that the relative strength of the emissions can be plotted as a function of photon energy.

In Figure 2 the relative strengths of the emission features are compared to the calculated absorption strengths. In all cases, the experimental emission strength is taken as the peak height since the natural linewidths are significantly greater than the experimental resolution at all energies. In the case of the Ce 5*p*, only one spin-orbit split component was used, and even then the magnitudes of the Ce 5*p* peaks were scaled down by a factor of three for the plots. Strong Auger emission in some photon energy ranges prevented reasonable estimates of direct emission strengths. With all of these provisos, the quantitative agreement over much of the energy range is surprisingly good. The notable deviation from the absorption cross sections is the increase in strength of the Ce 5*p* and loss of strength in the Ce 4*f* relative to the calculated absorption cross sections at higher energies. Since the binding energy of the Ce 5*p* is about 20 eV, the unpredicted strength of the Ce 5*p* emission does not cause a problem with the use of calculated absorption cross sections for identifying *f* character in the valence band.

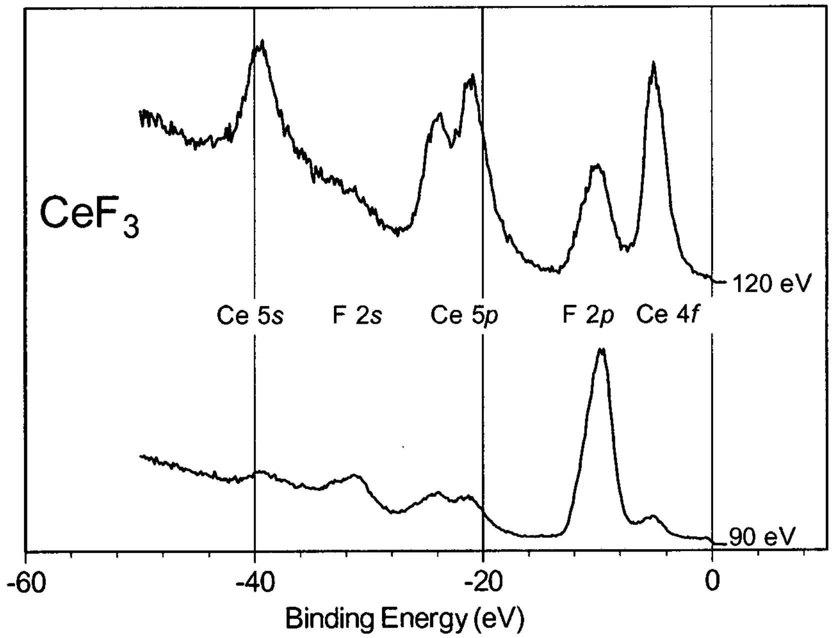

Figure 1. Energy Distribution Curves for CeF_3 before (90 eV) and at (120 eV) resonance. The atomic character of each of the peaks is indicated.

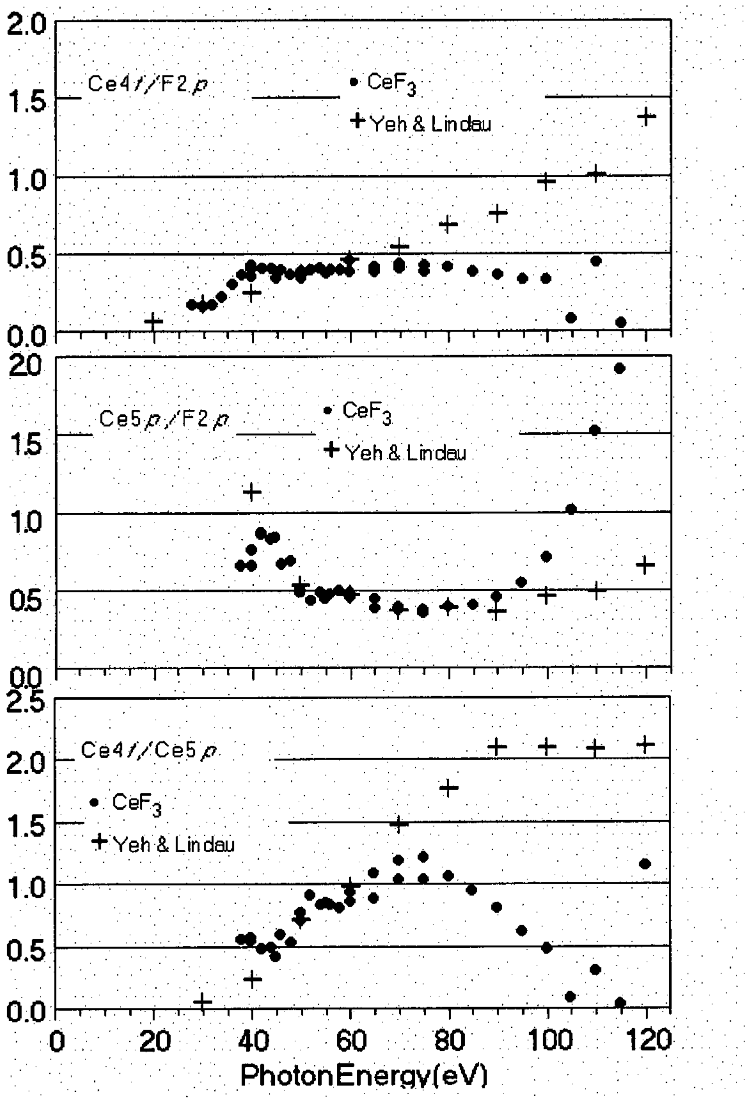

Figure 2. Relative strength of the experimental photoemission cross sections for atomic levels in CeF_3 compared to the calculated [1] absorption cross sections.

Resonance

The classic case of rare earth resonant photoemission involves the excitation of a core electron (4*d*) to a state that is well localized on the site of the core hole (4*f*). The excitation is not as well localized in the Actinides, but it is useful to look at what happens in the rare earths as localization decreases. The excitation of a 4*d* core to a 4*f* empty state can decay via Auger electron emission resulting in a vacancy in a 5*p*, 4*f* or 5*d* state. The same final state can result from direct emission of these valence electrons or shallow cores.[2] The interference between the two processes leads to resonant enhancement of the emission with details that are sensitive to the decay channels. While the 4f enhancement is very large, the other levels also show significant resonant enhancement as can be seen in Figure 1. Within the dipole approximation, photoemission accesses orbital components which are $\Delta\ell\pm1$ from the occupied states.

There are no occupied 5*d* electron states in CeF_3, but elemental Europium provides a good example of the relative response of *d* and *f* electrons at resonance. Europium normally forms in the bcc phase. Moderately thick layers can be produced in a meta stable phase that is probably fcc[3]. The resulting change in the angle-integrated EDCs is shown in Figure 3. In the bcc phase there is weak emission from 5*d* states at the Fermi level. The 4*f* and 5*p* cores show multiplet structures. In the meta stable phase, there is no strength at the Fermi level, and the 4*f* and 5*p* states no longer show multiplet structures. Hence, in the bcc phase we can look at resonance for a pure 5*d* state near the Fermi level, and for fcc, pure 4*f* and 5*p* at deeper binding energies.

The photon energy dependent spectra for the bcc phase are shown in Figure 4. The yield (approximately the absorption coefficient) shows the characteristic fine structure below threshold. Since Europium is 2+, the *f* count is the same as 3+ Gadolinium, and the fine structures are identical except for a photon energy shift. Also shown are the Constant Initial State spectra (CIS) for the binding energies of the 4*f* multiplet and the 5*d* states just below the Fermi level. CIS spectra are equivalent to taking a large number of EDCs as a function of photon energy and then plotting the intensity at a given binding energy as a function of photon energy. The important feature here is that the 5*d* state resonates at a slightly lower photon energy than the 4*f*. This is consistent with the model of Zangwell and Soven[4]. The detailed shape on the high energy side of the main peak will change with details of the final states and decay channels, but shift in position of the onset of the main peak is a durable indicator of d character. The 4*f* CIS spectra for bcc and fcc Europium are the same, so that in this case the *f* multiplet splitting has not modified the *f* resonant response

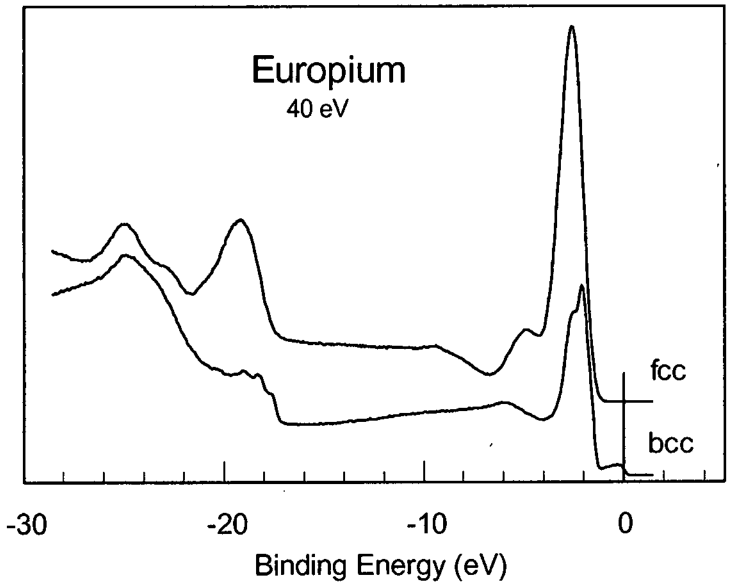

Figure 3. Energy Distribution Curves for the normal (bcc) and meta stable (fcc) phases of Europium.

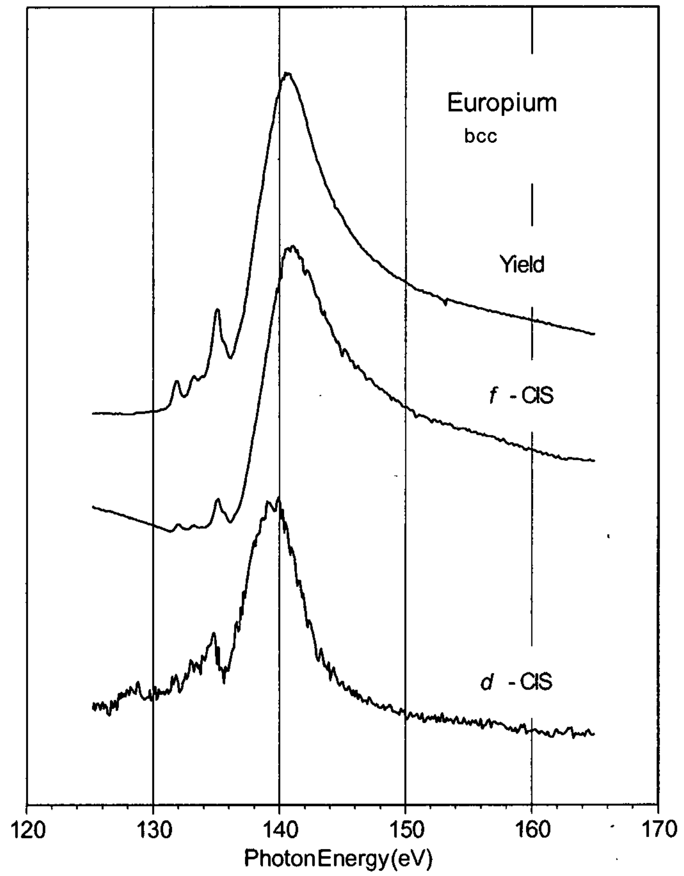

Figure 4. The photon energy dependence of the absorption coefficient and the direct emission intensity of the 4*f* and 5*d* initial states of Europium. The magnitudes of the spectra with respect to each other are arbitrary.

Systematics.

Another advantage in comparing the Actinides and Rare Earths are the systematics available from the full series of the rare earths. LaSb[5] provides another opportunity to look at the response of the 5*d* electrons at resonance without masking from 4*f* emission. Figure 5 shows the yield (essentially the absorption coefficient) of LaSb, as well as CIS spectra for significant initial state binding energies that will be identified in the following figure. The significant feature of the main resonance around 115 eV is that in the CIS data, the initial states (E_B) near the Fermi level resonate at a distinctly lower photon energy than the bulk of the valence band.

Another difference compared to Eu is that La has a simple 4*d* – 4*f* multiplet structure with only a single strong fine structure peak below the main resonance threshold. This gives us an opportunity to look at resonant effects with a change in photon energy of only 0.5 eV, minimizing the change in any Sb component in the valence band or any change due to crystal momentum differences. In the left panel of Figure 6, the upper EDC at each angle is at 101.5 eV (on resonance) and the lower EDC is at 102 eV (off resonance). The existence of a small amount of 5*d* character is clear in the difference curves in the right panel.

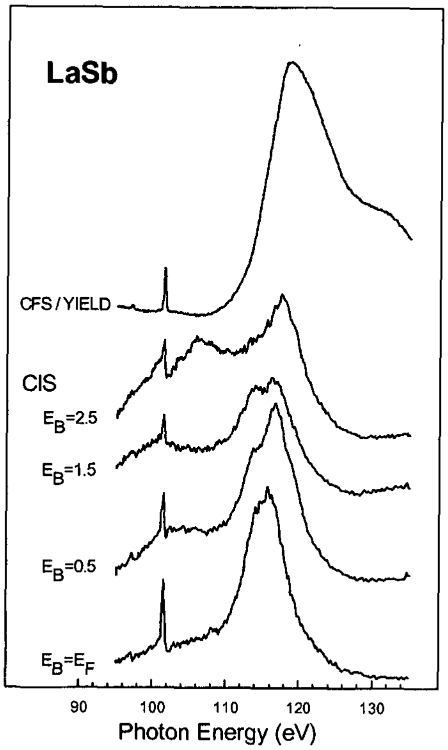

Figure 5. The photon energy dependence through resonance of the absorption coefficient and direct emission intensities of selected initial states in the valence band. The additional structure (beyond the 4d-4f single peak fine structure) between 100 and 110 eV in the CIS spectra is the consequence of the Sb 4p core level.

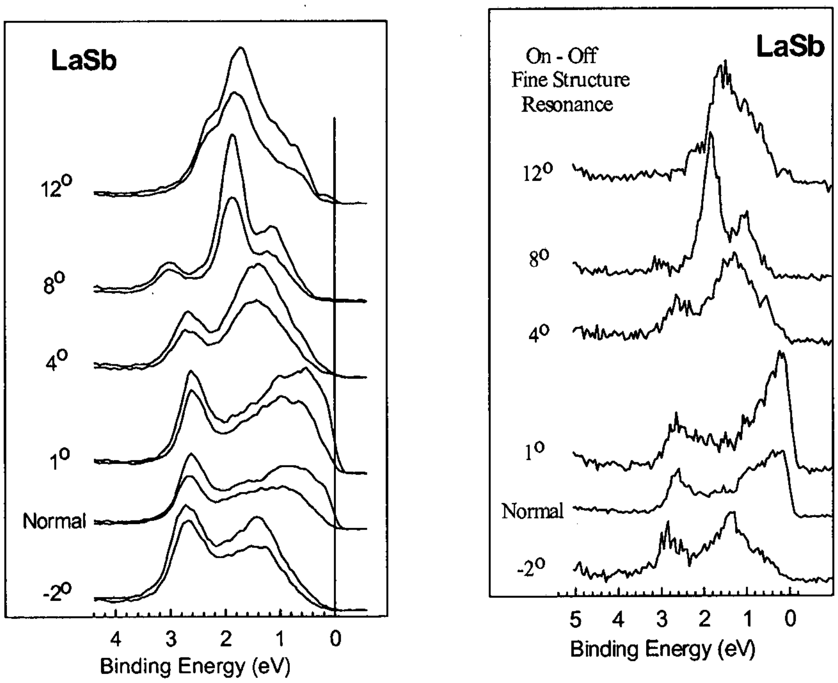

Figure 6. Left panel: At each angle, the upper EDC is on resonance (101.5 eV) and the lower EDC is off resonance (102 eV). The difference between the two spectra are displayed in the right panel.

DISCUSSION

The effect of f character in the valence band and the result of *f-d* hybridization can be seen by comparing the four light rare earths antimonides to USb in Figure 7. LaSb has no filled *f* levels, and in NdSb the *f* states are below the valence band. The spectra are equivalent except for a small increase in the valence band width. For CeSb and PrSb the valence band states are modified, CeSb primarily just below the Fermi energy (E_F), and for PrSb a little deeper in binding energy. This is suggestive of being the result of hybridizations with the *f* levels. Only the influence of the *f* electrons on the valence band is seen since *f* electrons have a very low cross section for emission at this energy and they are not observed directly. USb is notable for the broadened valence band structures and the increased strength at the Fermi level. The 22 eV EDCs are from a point along the line between Γ and X. These spectra represent what would be seen with a He I source. This is a useful photon energy since it minimizes the *f* character, but it does not sample a high symmetry point in the Brillion zone.

A much more complete picture of the valence band electronic structure can be seen in the full range of spectra from Γ to X shown in Figure 8. Here USb[6] is compared to CeSb, which is its closest rare earth analog in electronic properties (least bound f-electron), and NdSb which has the same formal *f* count. The striking difference in USb relative to CeSb is the strength at the Fermi level. The X point is reached for USb in normal emission at 33 eV for states at the Fermi level. [Do we want to make a centripetal barrier statement and relate it to 4f vs. 5f cross-sections at this point ??] At this photon energy the *f* cross section for emission is appreciable, and the single EDC cannot differentiate *f* and *d* character. At the lowest photon energies shown, the *f* cross section is very small, and the remnant strength in the first few meV is more likely to be *d*. This, however, is at Γ, so a direct comparison to an arbitrary higher photon energy is not possible.

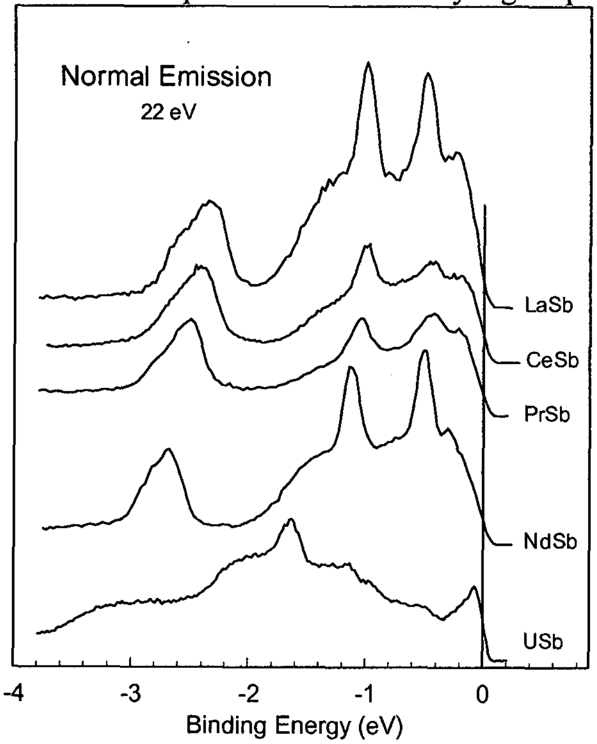

Figure 7. Angle-Resolved normal emission EDCs for the light rare earths and USb.

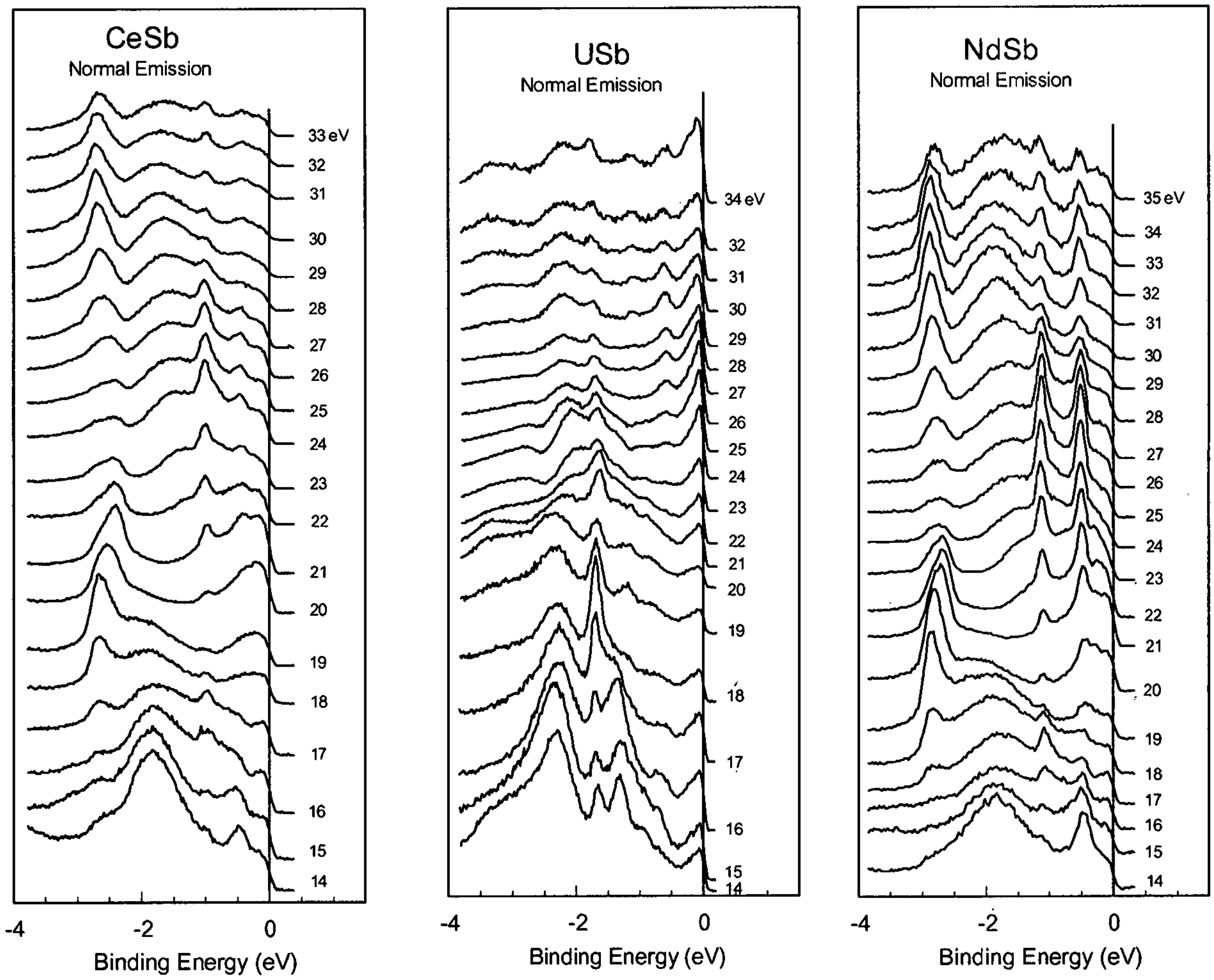

Figure 8. Angle-resolved normal emission EDCs for CeSb, USb and NdSb. The lowest photon energy corresponds to crystal momenta at the Γ point, and the highest photon energy samples the X point.

It is possible in general, and for USb in particular, to compare equivalent high symmetry points in the Brillion zone under conditions in which changes in cross section will give detailed information. The X point can be reached at low photon energies by going off-normal to another X point in the extended zone scheme. In addition, increasing the photon energy in normal emission will access the next X point at greater perpendicular momentum. In this case we get lucky. The appropriate photon energy is very near a small fine structure resonance which we will consider in more detail in the next figure. This fine structure allows us to take EDCs at the X point, with and without 5*d* resonant enhancement as was done for LaSb. The result in Figure 9 is that we can show that there is Uranium 5*f* and 6*d* strength at the Fermi level, and through the first 600-800 meV. The much stronger response of the 5*f* to resonance will dominate at the highest photon energy. The 33.5 eV EDC is a combination of 5*f* and 6*d* emission, but the 17 eV EDC shows the sizeable amount of 6*d* character at the Fermi level at the X point. Systematic studies such as this[6] show that the Uranium 6*d* character is greatest near the X point.

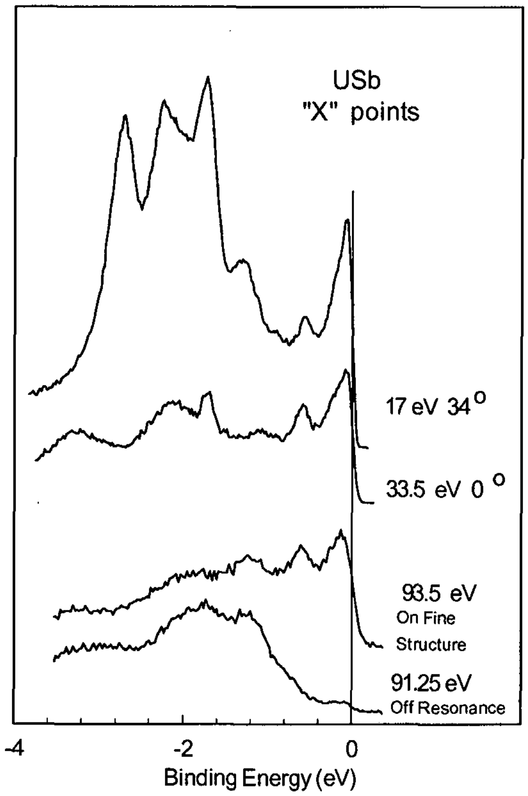

Figure 9. EDCs at three equivalent points in the extended zone scheme showing the changes due to the photon energy dependence of the cross sections. The difference between the 93.5 eV on resonance spectrum and the 91.25 eV off-resonance spectrum is attributable to the Uranium derived states near the Fermi level.

The conclusion that there is Uranium 6*d* character (as well as 5f character) at the Fermi level is reinforced by the spectra in Figure 10. Here the yield and CISs for binding energies near the Fermi level for USb are compared to amorphous (polycrystalline?) UPt_3 as an example of a material with predominantly 5*f* states at the Fermi level. The USb spectra are complicated by the background due to the Sb 4*p* core, but the shift of the resonance to lower photon energy is clear. Again, for USb this resonance photon energy is sampling the X symmetry point where 6*d* character is the largest. The weak structure near 93.5 eV is the fine structure that was utilized to isolate the Uranium character in Figure 9.

Another lesson from the rare earths is that the primary effect of *f-d* hybridization on the otherwise extremely sharp fine structure is to broaden the structures and redistribute the relative strengths rather than cause energy shifts[7]. The washed out fine structure in USb is further evidence of 5*f*-6*d* hybridization.

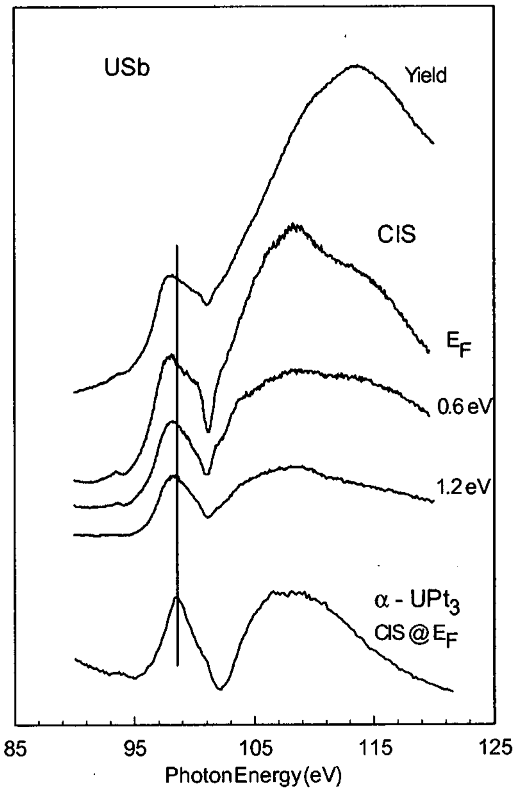

Figure 10. The absorption coefficient of USb and CIS spectra from initial states near the top of the valence band. The shift of the onset of the main peak to lower photon energy with respect to the dominant *5f* response of amorphous UPt_3 is an indication of Uranium *6d* character near the Fermi level.

CONCLUSIONS

Angle-resolved photoemission over a wide range of photon energies can be used to extract detailed information about the atomic character of valence band states in Actinides. We have shown that there is mixed *5f*-*6d* character at and near the Fermi level in USb and that the greatest *6d* density is near the X point.

ACKNOWLEDGEMENT

The Ames Laboratory is operated by Iowa State University for the U.S. Department of Energy under Contract No. W-7405-ENG-82. The work at Los Alamos National Laboratory was supported by the U.S. Department of Energy, Office of Science, Division of Materials Science and Engineering. This work is based upon research conducted at the Synchrotron Radiation Center, University of Wisconsin-Madison, which is supported by the NSF under Award No DMR-0084402.

REFERENCES

1. J.J. Yeh and I. Lindau, At. Data Nucl. Data Tables 32, 1 (1985)

2. See for example: J.W. Allen, in R.Z. Bachrach (Ed.), Synchrotron Radiation Research: Advances in Surface and Interface Science, Vol. 1; Techniques, Plenum Press, New York, 1992, p. 253.

3. C.G. Olson, X. Wu, S-L. Chen and D.W. Lynch, Phys. Rev. Lett. **74**, 992 (1995).
4. A.Zangwill and Paul Soven, Phys. Rev. Lett. 45, 204 (1980).

5. C.G. Olson, P.J. Benning, M. Schmidt, D.W. Lynch, P. Canfield and D.M. Wieliczka, Phys. Rev. Lett. **76** 4265 (1996).

6. USb paper to follow

7. D.W. Lynch and R.D. Cowan, Phys. Rev. B, **36**, 9228 (1987) and C. G. Olson, S.J. Chase, P. Canfield and D.W. Lynch, J. of Elec. Spec. and Rel. Phenom., **93**, 175 (1998).